

Modern Physics Letters A  
 © World Scientific Publishing Company

## DO THE FUNDAMENTAL CONSTANTS CHANGE WITH TIME ?

NISSIM KANEKAR

*National Radio Astronomy Observatory, 1003 Lopezville Road, Socorro, NM 87801, USA  
 nkanekar@nrao.edu*

Comparisons between the redshifts of spectral lines from cosmologically-distant galaxies can be used to probe temporal changes in low-energy fundamental constants like the fine structure constant and the proton-electron mass ratio. In this article, I review the results from, and the advantages and disadvantages of, the best techniques using this approach, before focussing on a new method, based on conjugate satellite OH lines, that appears to be less affected by systematic effects and hence holds much promise for the future.

*Keywords:* Line: profiles – techniques: spectroscopic – radio lines

PACS Nos.: 98.80.Es,06.20.Jr,33.20.Bx,98.58.-w

### 1. Introduction

In modern higher-dimensional extensions of the standard model of particle physics, low-energy fundamental constants like the fine structure constant  $\alpha$ , the proton-electron mass ratio  $\mu \equiv m_p/m_e$ , etc, are expected to be dynamical quantities that show spatio-temporal evolution (e.g. [1, 2]). The detection of such changes provides an avenue to explore new physics, especially important because most other predictions of these models lie at inaccessibly high energies ( $\gtrsim 10^{19}$  GeV). However, the timescales of these putative changes are unknown, implying that it is necessary to search for evolution over as wide a range of timescales as possible (especially as it is not even clear that any evolution will be monotonic). It is also important to probe changes in different constants: fractional changes in  $\mu$  are expected to be far larger than those in  $\alpha$ , by factors of  $\sim 50 - 500$  (e.g. [3, 4]).

On short timescales (a few years), laboratory experiments, usually based on frequency comparisons between atomic clocks and other optical frequency standards have provided the strongest constraints on changes in (especially) the fine structure constant. For example, a recent comparison between  $^{199}\text{Hg}^+$  and  $^{27}\text{Al}^+$  clocks found  $\dot{\alpha}/\alpha < 4.6 \times 10^{-17} \text{ yr}^{-1}$  over one year [5]. In the case of the proton-electron mass ratio, [6] obtained  $\dot{\mu}/\mu < 1.2 \times 10^{-13} \text{ yr}^{-1}$ , comparing frequencies derived from molecular and cesium clocks over a two-year period. Note that all limits quoted in this paper are at  $2\sigma$  significance.

Besides the impressive precision of these (and other) laboratory results, it should be noted that they allow direct control over systematic effects. Unfortunately, they

2 *Nissim Kanekar*

are limited to probing changes in the constants over timescales of only a few years. Various geological methods have allowed the extension of such studies to lookback times of a few billion years; most prominent amongst these are measurements of relative isotopic abundances in the Oklo natural fission reactor and studies of the time variation of the  $\beta$ -decay rate (e.g. [7]). However, while sensitive constraints on changes in  $\alpha$  (over  $\sim 1.8-4$  Gyr) have been obtained from both these methods, they typically are model-dependent and involve assumptions about the constancy of other parameters (e.g. [8, 9, 10]). For example, [9] obtain the  $2\sigma$  limit  $-0.24 \times 10^{-7} < [\Delta\alpha/\alpha] < 0.11 \times 10^{-7}$  from a re-analysis of Oklo nuclear yields, but emphasize that this depends critically on the assumption that  $\alpha$  alone changes with time; any changes in the nuclear potential could significantly affect the result.

Astrophysical techniques allow tests of changes in the fundamental constants over large lookback times, out to significant fractions of the age of the Universe. The methods can be broadly divided into the following three categories: (1) measurements of the abundances of elements formed during Big Bang nucleosynthesis (BBN) [11], (2) observations of anisotropies in the cosmic microwave background [12, 13] and (3) comparisons between the redshifts of spectral lines from distant galaxies [14]. The first two of these probe the largest lookback times, but the results are not very sensitive due to degeneracies with the cosmological parameters, which are not *a priori* known (e.g. [15]). Additionally, most BBN studies are highly model-dependent as the dependence of the nuclear binding energies on the fundamental constants is still not known [16]. In this article, I will concentrate on the third category, the use of astronomical spectroscopy to probe changes in three constants,  $\alpha$ ,  $\mu \equiv m_p/m_e$  and the proton g-factor ratio  $g_p$  (or combinations of these quantities). After discussing the results from, and advantages and disadvantages of, the main techniques currently used in this endeavour, I will focus on a new technique, based on “conjugate” satellite hydroxyl (OH) lines, that appears to be less affected by systematic effects. Finally, I will discuss prospects for such studies of fundamental constant evolution, based on new telescopes and instruments over the next decade.

## 2. Redshifted spectral lines: background

The idea that comparisons between the velocities of different transitions arising in a distant galaxy might be used to test for spatio-temporal dependences in the fundamental constants was first suggested more than half a century ago [14] and is conceptually quite simple. Different spectral transitions arise from different physical mechanisms (e.g. interactions of fine structure, hyperfine structure, rotational or other types) and the line frequencies have different dependences on the fundamental constants. For example, hyperfine line frequencies are proportional to  $g_p\mu\alpha^2$ , while rotational line frequencies are proportional to  $\mu$ . If the fundamental constants are different at different space-time locations (e.g. in external galaxies), the rest frequency of a transition would be different at these locations from the value measured in terrestrial laboratories. Different spectral transitions arising in a given gas cloud

(or galaxy) would then yield different systemic velocities, as the incorrect (laboratory) rest frequency would be used for each line to estimate the cloud velocity. A comparison between the line velocities and the known dependence of the line rest frequency on the constants can then be used to determine the fractional change in a given constant between the space-time locations of the cloud and the Earth. For example, a comparison between hyperfine and rotational velocities is sensitive to changes in  $g_p\alpha^2$ , and one between hyperfine and fine structure transitions, to changes in  $g_p\mu\alpha^2$ . Most such studies are carried out in absorption (or stimulated emission), against distant quasars, because absorption lines can be detected out to high redshifts with undiminished intensity and are also usually much narrower than emission lines, allowing precision measurements of the line redshift (but see [17]).

A critical assumption here is that an observed velocity offset between different transitions can be ascribed to changes in the fundamental constants, i.e. that “local” velocity offsets (e.g. due to motions within galaxies or clouds) are negligible. This is manifestly incorrect as transitions from different species often arise from different parts of a gas cloud, at different velocities. Even transitions from one species need not arise at the same velocity, if the cloud is not in equilibrium. Intra-cloud velocities of  $\sim 10$  km/s are common in astrophysical circumstances; these would yield systematic effects of order  $(v/c) \sim \text{few} \times 10^{-5}$  on estimates of fractional changes in the constants (e.g. [18, 19]). As will be seen later, the best present estimates of fractional changes in  $\alpha$  and  $\mu$  are of this order, implying that such local offsets cannot be neglected. Two approaches have been used to handle such systematics: (1) a statistically-large sample of spectral lines, to average out local effects (e.g. the many-multiplet method; [20]) and (2) the use of certain spectral lines, where the physics of the line mechanism causes such local effects to be negligible (e.g. the conjugate satellite OH approach; [21, 22]).

### 3. Optical techniques

Most studies of fundamental constant evolution based on redshifted spectral lines have used optical techniques, partly, no doubt, due to the profusion of strong ultraviolet transitions that are redshifted into optical wavebands. The three principal approaches are:

#### 3.1. Alkali doublet method

For three decades, redshifted alkali doublet (AD) lines provided the main spectroscopic probe of the long-term evolution of the fine structure constant (e.g. [23, 24]). The fractional separation between the doublet wavelengths is proportional to  $\alpha^2$  and the measured line redshifts thus directly provide an estimate of  $[\Delta\alpha/\alpha]$  [14]. The best present result from this technique is  $[\Delta\alpha/\alpha] < 2.6 \times 10^{-5}$ , based on High Resolution Echelle Spectrograph (HIRES) absorption spectra of 21 SiIV doublets at  $2 < z < 3$ , with the Keck telescope [25]. While [26] obtained  $[\Delta\alpha/\alpha] < 0.86 \times 10^{-5}$  from Very Large Telescope Ultraviolet Echelle Spectrograph (VLT-UVES) spectra

of 15 SiIV doublets at  $1.6 < z < 2.9$ , it has been pointed out that their  $\chi^2$  curves contain large fluctuations, making the result unreliable [27]. Although the sensitivity of the AD method is nearly an order of magnitude poorer than that of the many-multiplet method (discussed next), the fact that the two doublet lines have the same shape provides a useful test for systematic effects. Further, the doublet lines lie at nearby wavelengths, and hence usually on the same echelle order, implying that relative wavelength calibration across orders is not an issue. [28] note that differential isotopic saturation of the SiIV lines must be taken into account when using saturated lines in this method; even better would be to restrict the analysis to unsaturated SiIV absorbers alone.

### 3.2. *The many-multiplet method*

The many-multiplet (MM) method, devised by [20], is based on the fact that relativistic first-order corrections imply that the wavelengths of fine structure transitions in different species have different dependences on  $\alpha$ . Thus, unlike the AD method, the MM method is based on comparisons between transitions from *different* species and hence must be carried out on large absorber samples to average out local effects. This has resulted in a significant improvement in sensitivity to fractional changes in  $[\Delta\alpha/\alpha]$  over the alkali doublet approach, albeit perhaps with a concomitant increase in systematic effects (see, e.g., [17, 28, 29, 30]). This is also, at present, the only technique that finds evidence for a change in the fine structure constant: [31] used Keck-HIRES data to obtain  $[\Delta\alpha/\alpha] = [-0.573 \pm 0.113] \times 10^{-5}$  from 143 absorbers in the redshift range  $0.2 < z < 4.2$ , implying that  $\alpha$  was smaller at earlier times (see also [29]). A slew of later VLT-UVES observations have claimed strong constraints on  $[\Delta\alpha/\alpha]$ , from either the MM method or its variants (e.g. the SIDAM method; [32, 33]), some of which are inconsistent with the Keck-HIRES result (e.g. [34]). For example, [30, 33] use the SIDAM method to obtain  $[\Delta\alpha/\alpha] = (5.7 \pm 2.7) \times 10^{-6}$  and  $[\Delta\alpha/\alpha] = (-0.12 \pm 1.79) \times 10^{-6}$  from absorbers at  $z \sim 1.84$  and  $z \sim 1.15$ , respectively. However, [27] point out that the  $\chi^2$  curves of [34] show large fluctuations, causing them to under-estimate their errors by a factor of  $\gtrsim 3$ . [27] also argue that some of the other VLT-UVES results are likely to be unreliable, notably due to the fitting of insufficient components [32, 33]. Conversely, [30] find non-gaussian tails in the distribution of the Keck-HIRES data of [29, 31], as well as correlations in the data, suggesting that they too may have under-estimated their errors.

Excellent discussions of the systematic effects inherent in the MM (and AD) methods are provided by [28, 29], who find no evidence that their Keck-HIRES result may be affected by such systematics (but see [30]). Isotopic abundance variation with redshift is perhaps the most important source of systematic effects in the MM method, as lines from multiple isotopes are blended for most species (especially Mg), and terrestrial isotopic abundances are assumed in order to determine the central line wavelength [31, 35]. For example, higher  $^{25,26}\text{Mg}$  fractional abundances

in the  $z < 1.8$  sample of [31] could yield the observed negative  $[\Delta\alpha/\alpha]$  for this sample. Interestingly enough, [30] find that the results of [29, 31] appear to be dominated by the sample that uses MgII lines: the sub-sample of [29] that uses the MgII lines yields a  $\beta$ -trimmed mean of  $[\Delta\alpha/\alpha] = (-0.48 \pm 0.12) \times 10^{-5}$ , while the sub-sample without these lines gives  $[\Delta\alpha/\alpha] = (-0.11 \pm 0.17) \times 10^{-5}$  [30]. Further, the isotopic structure is only known for a few of the transitions (e.g. Mg, Si) used in the full analysis [25]. Unfortunately, it will be difficult to resolve this issue by direct observations, while indirect arguments depend on the details of galactic chemical evolution models [35, 36].

Other sources of systematics in the MM method include the assumption that all species have the same kinematic structure and the possibilities of line blends and line misidentifications (e.g. [17, 28, 29]). As emphasized by [28], these are likely to result in random contributions to  $[\Delta\alpha/\alpha]$ . However, it is unclear whether the number of systems is sufficient to cancel such systematic effects at the level of  $(v/c) \sim 0.1$ , i.e.  $\Delta v \sim 0.3$  km/s [17]. Note that the SIDAM method does not require the assumption that different species have the same velocity structure [30], an advantage over the original MM method. Finally, the fact that the transitions used in the MM and SIDAM methods lie at rest-frame ultraviolet wavelengths has meant that it is difficult to apply these to Galactic lines of sight, to test whether the expected null result is obtained at  $z = 0$ .

### 3.3. Molecular hydrogen lines

The numerous ultraviolet ro-vibrational transitions of molecular hydrogen ( $\text{H}_2$ ) have different dependences on the reduced molecular mass, implying that comparisons between the line redshifts can be used to probe changes in  $\mu$  [37, 38]. Unfortunately, these lines are both weak and, for redshifted absorbers, lie in the Lyman- $\alpha$  forest, making them difficult to detect. As a result, only about a dozen redshifted  $\text{H}_2$  absorbers are presently known, of which only three have been useful in studying changes in  $\mu$  (e.g. [38, 39, 40]). While all earlier studies had provided constraints on  $[\Delta\mu/\mu]$ , [39] used VLT-UVES observations of two of these systems to obtain  $[\Delta\mu/\mu] = (2.0 \pm 0.6) \times 10^{-5}$  over  $0 < z < 3$ , i.e.  $3.5\sigma$  evidence for a larger value of  $\mu$  at early times. A recent re-analysis of the same data, combined with VLT-UVES data on the third absorber, at  $z \sim 2.811$  towards PKS 0528–25, has yielded the strong constraint  $[\Delta\mu/\mu] < 6.0 \times 10^{-6}$  [40]. However, the new (high-sensitivity) data towards PKS 0528–25 show a complicated velocity structure and the result could be affected by the presence of unresolved spectral components. In addition, [40] choose to carry out a simultaneous fit to the  $\text{H}_2$  profiles as well as all Lyman- $\alpha$  forest transitions near the  $\text{H}_2$  lines, rather than excluding possible blends with Lyman- $\alpha$  forest interlopers (as is usually done; e.g. [39]). While this allowed them to retain a far larger number of  $\text{H}_2$  lines in the analysis, it is unclear what effect it might have for their results. Again, it has not been possible to test that this method yields the expected null result in the Galaxy.

#### 4. Radio techniques

The methods discussed in the preceding section were all based on optical spectroscopy, where relative wavelength calibration of echelle orders, line blending due to the low spectral resolution ( $\sim 6 - 8$  km/s), local velocity offsets, line interlopers, etc, are all possible sources of systematic error (e.g. [29]). The many-multiplet method is affected by the additional problem of unknown isotopic abundances at high redshift, while fits to redshifted  $H_2$  transitions must be carried out in the fog of the Lyman- $\alpha$  forest. Given the possibility that under-estimated or unknown systematics might dominate the errors from a given technique, it is important that independent techniques, with entirely different systematic effects, be used.

Different radio transitions arise from very different physical mechanisms (e.g. hyperfine splitting, molecular rotation, Lambda-doubling, etc) and the line frequencies hence have different dependences on the fundamental constants. Comparisons between the redshifts of radio lines (or between radio and optical lines; [41]) can thus be used to probe changes in the fundamental constants, with the immediate benefit that systematic effects are very different in the radio regime. Obvious advantages over optical techniques are the high spectral resolution ( $< 1$  km/s) possible at radio frequencies, alleviating problems with line blending, and the fact that the frequency scale is set by accurate masers and local oscillators, allowing frequency calibration to better than  $\sim 10$  m/s. Further, comparisons between the redshifts of multiple transitions from a single molecule (e.g. OH,  $NH_3$ , CH), with different dependences on the constants, reduces the likelihood that the result might be affected by local velocity offsets in the gas cloud between the lines.

##### 4.1. *The HI 21cm hyperfine transition*

The HI 21cm hyperfine transition is the most commonly detected radio line at cosmological distances and is hence used in a number of comparisons to probe changes in the fundamental constants. [41] were the first to use the HI 21cm line for this purpose, comparing HI 21cm and metal-line (MgII) absorption redshifts in a  $z \sim 0.524$  absorber to constrain evolution in the quantity  $X \equiv g_p \mu \alpha^2$ . More recently, [42] used a similar comparison to obtain  $[\Delta X/X] < 2 \times 10^{-5}$  from nine redshifted HI 21cm absorbers at  $0.23 < z < 2.35$ . An obvious concern about this measurement is that [42] compared the redshifts of the deepest HI 21cm and metal-line absorption components, assuming that these arise in the same gas. However, many of the systems used in [42] have multiple components in both HI 21cm and metal transitions and it is by no means necessary that the strongest absorption arises in the same component in both types of lines [43].

Comparisons between the redshifts of the HI 21cm and molecular rotational transitions (e.g. CO,  $HCO^+$ ) are sensitive to changes in  $Y \equiv g_p \alpha^2$ . At present, there are just four redshifted systems with detections of both HI 21cm and rotational molecular absorption (e.g. [18, 44]), of which only two are suitable to probe changes in the constants. [19] used these to obtain  $[\Delta Y/Y] < 3.4 \times 10^{-5}$  from  $z \sim 0.25$

and  $z \sim 0.685$ , conservatively assuming that differences between the HI 21cm and millimetre sightlines could yield local velocity offsets of  $\sim 10$  km/s.

An important source of systematic effects in both these techniques is that the background quasar is far larger at the low redshifted HI 21cm frequencies ( $\lesssim 1$  GHz) than at the millimetre wavelengths of the strong rotational transitions or the optical fine structure lines. This implies that the sightlines in the different transitions could probe different velocity structures in the absorbing gas. For example, large velocity offsets ( $\sim 15$  km/s) have been observed between the HI 21cm and HCO<sup>+</sup> redshifts at  $z \sim 0.674$  towards B1504+377, probably due to small-scale structure in the absorbing gas [45, 44, 46]. This is less of an issue for a comparison between the HI 21cm and “main” OH 18cm lines, which is sensitive to changes in  $Z \equiv g_p[\mu\alpha^2]^{1.57}$  [47]. [48] used four HI 21cm and OH 18cm spectral components in two gravitational lenses to obtain  $[\Delta Z/Z] < 2.1 \times 10^{-5}$  from  $z \sim 0.7$ , assuming possible systematic velocity errors of  $\sim 3$  km/s between the HI 21cm and OH components. The strong dependence of  $Z$  on  $\alpha$  ( $Z \propto \alpha^{3.14}$ ) implies that this comparison is very sensitive to changes in  $\alpha$ , with a  $2\sigma$  sensitivity of  $[\Delta\alpha/\alpha] < 6.7 \times 10^{-6}$  [48].

#### 4.2. Ammonia inversion transitions

An interesting technique to probe changes in the proton-electron mass ratio, using inversion transitions of the ammonia (NH<sub>3</sub>) molecule, was proposed by [49]. The dependence of the NH<sub>3</sub> inversion frequency on  $\mu$  is far stronger than that of rotational line frequencies, implying that a comparison between NH<sub>3</sub> and (for example) CO redshifts in an absorber can yield a high sensitivity to changes in  $\mu$ . Recently, [50] used NH<sub>3</sub> and rotational (HCO<sup>+</sup> and HCN) lines in the  $z \sim 0.685$  gravitational lens towards B0218+357 to obtain  $[\Delta\mu/\mu] < 1.8 \times 10^{-6}$  over  $\sim 6.5$  Gyr. While this is the most sensitive single bound on changes in  $\mu$ , the analysis assumes the same velocity structure in the NH<sub>3</sub> and rotational lines (8 spectral components), despite the fact that there is no evidence for more than 2 components in the NH<sub>3</sub> spectra [51]. It is unclear what effect this might have on the results. Further, the NH<sub>3</sub> lines are assumed to be in local thermodynamic equilibrium, so that the eighteen components of the NH<sub>3</sub> 1-1 multiplet have the same velocity width; it is not possible to verify this at the low signal-to-noise ratio (S/N) of the present NH<sub>3</sub> spectrum. The quasar image (“A”; [52]) that shows strong molecular absorption is also only partly obscured at optical wavelengths (remaining clearly visible), despite the high extinction of the foreground molecular cloud. This indicates structure in the molecular cloud on the very small scales of the optical quasar [52], which could lead to different velocity structures in the NH<sub>3</sub> and HCO<sup>+</sup> lines, due to their very different line frequencies ( $\sim 23.7$  GHz and  $\sim 178.4$  GHz, in the absorber’s rest frame; [50]). In addition, the analysis assumes no local velocity offsets between the NH<sub>3</sub> and rotational lines. As always, comparisons between lines from different species require large absorber samples to average out such effects.

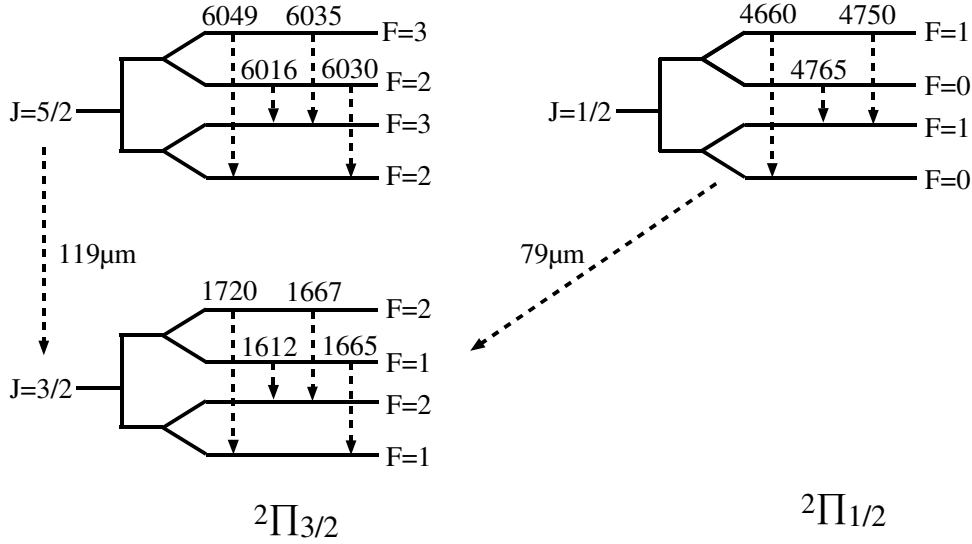
8 *Nissim Kanekar*


Fig. 1. The 3 lowest rotational OH states (not to scale) and their microwave and infra-red lines.

### 5. “Conjugate” Satellite OH lines

The satellite OH 18cm lines are said to be conjugate when the two lines have the same shape, but with one line in emission and the other in absorption. This arises due to an inversion of the level populations within the ground state of the OH molecule [53, 54]. For clarity, Fig. 1 shows the three lowest OH rotational states (not to scale). The  $2\Pi_{3/2}$  J=3/2 OH ground rotational state (and every excited OH state) is split up into four sub-levels by  $\Lambda$ -doubling and hyperfine splitting; transitions between these sub-levels give rise to the microwave OH spectrum. Transitions with  $\Delta F = 0$ , i.e. with no change in the total angular momentum quantum number  $F$ , are referred to as “main” lines, while transitions with  $\Delta F = \pm 1$  are called “satellite” lines. The rest frequencies of the ground state lines are known to high accuracy, with the main lines at 1665.401803(12) MHz and 1667.358996(4) MHz [55], and the satellite lines at 1612.230825(15) MHz and 1720.529887(10) MHz [56].

If the OH molecules are pumped from the ground state to higher rotational states, either collisionally or radiatively, they cascade back down to the ground state. The last step of the cascade can be either the  $119\mu\text{m}$  intra-ladder transition,  $2\Pi_{3/2}$  (J=5/2)  $\rightarrow$   $2\Pi_{3/2}$  (J=3/2) or the  $79\mu\text{m}$  cross-ladder transition,  $2\Pi_{1/2}$  (J=1/2)  $\rightarrow$   $2\Pi_{3/2}$  (J=3/2). Both decays are governed by the quantum mechanical selection rules  $\Delta F = 0, \pm 1$ . For the  $119\mu\text{m}$  route, this means that transitions from the  $F = 3$  sub-levels of the excited state to the  $F = 1$  sub-levels of the ground state are forbidden, while the  $F = 2$  sub-levels can decay to all ground state sub-levels. Conversely, for the  $79\mu\text{m}$  route, transitions between the  $F = 1$  excited state sub-levels and the  $F = 3$  ground state sub-levels are forbidden, while all other transitions are allowed. Further, if the  $119\mu\text{m}$  or  $79\mu\text{m}$  transitions are op-



tically thick (requiring  $N_{\text{OH}} \gtrsim 10^{15} \text{ cm}^{-2}$ ; [53]), the sub-level populations in the ground state are determined only by the number of possible routes to each sub-level [53]. Thus, a cascade ending with an optically-thick  $119\mu\text{m}$  decay will result in an over-population of the  $F = 2$  ground state sub-levels, while one ending in an optically-thick  $79\mu\text{m}$  decay will yield an over-population of the  $F = 1$  sub-levels. Neither of these would have any effect on the ground state “main” lines, as the latter connect sub-levels with the same total angular momentum. However, the situation is very different for the satellite lines, connecting states with different  $F$  values. The first case (an optically-thick  $119\mu\text{m}$  decay), would result in stimulated 1720 MHz emission and 1612 MHz absorption, while the second case (an optically-thick  $79\mu\text{m}$  decay) would give rise to 1612 MHz emission and 1720 MHz absorption. In both cases, the satellite lines would also have the same shapes, implying that the sum of the satellite optical depths would be consistent with noise [53, 54].

Such “conjugate” satellite behaviour has been seen in nearby extra-galactic systems for more than a decade (e.g. Centaurus A; [54]) but has only recently been discovered at cosmological distances [21, 22, 48]. This is extremely useful for studies of fundamental constant evolution because the four OH 18cm transition frequencies have very different dependences on  $\alpha$ ,  $\mu$  and  $g_p$  [47]. Specifically, a comparison between the sum and difference of satellite line redshifts probes changes in the quantity  $G \equiv g_p [\mu\alpha^2]^{1.85}$  [47], with a high sensitivity to changes in both  $\alpha$  and  $\mu$  (a similar analysis by [57] implicitly assumes no changes in  $\mu$  and  $g_p$ ). Note that [21, 47] define  $\mu \equiv m_e/m_p$ ; the more common  $\mu \equiv m_p/m_e$  is used here.

Only two redshifted conjugate satellite OH systems are currently known, at  $z \sim 0.247$  towards PKS 1413+135 [21, 22] and  $z \sim 0.765$  towards PMN J0134–0931 [48]. We have recently carried out deep observations of the satellite OH lines of PKS 1413+135 with the Westerbork Synthesis Radio Telescope (WSRT) and the Arecibo telescope [58]. The WSRT and Arecibo optical depth spectra have root-mean-square noise values of  $\sim 8.5 \times 10^{-4}$  per  $\sim 0.55 \text{ km/s}$  and  $\sim 7 \times 10^{-4}$  per  $\sim 0.36 \text{ km/s}$ , respectively, after Hanning smoothing and re-sampling. These correspond to  $S/N \sim 1200$  at a resolution  $R \sim 550000$  and  $S/N \sim 1430$  at  $R \sim 830000$ ; for comparison, the 143 Keck-HIRES spectra of [31] typically had  $S/N \sim 30$  at  $R \sim 45000$ . The sum of the 1612 and 1720 MHz optical depth profiles was found to be consistent with noise in both data sets, as expected for conjugate behaviour, with no evidence for a velocity offset between the satellite lines. Our preliminary result from a cross-correlation analysis of the two data sets is  $[\Delta G/G] < 1.1 \times 10^{-5}$ , where  $G \equiv g_p [\mu\alpha^2]^{1.85}$ , consistent with no changes in  $\alpha$ ,  $\mu$  and  $g_p$  from  $z \sim 0.247$  to the present epoch. Assuming that changes in  $g_p$  are much smaller than those in  $\alpha$  or  $\mu$  (e.g. [4]), this gives  $2\sigma$  sensitivities of  $[\Delta\alpha/\alpha] < 3.1 \times 10^{-6}$  or  $[\Delta\mu/\mu] < 6.2 \times 10^{-6}$ , over  $0 < z < 0.247$ . The data are now being inspected for possible systematic effects.

We have also applied this technique to OH 18cm data from a nearby conjugate satellite system, Centaurus A [54]. Here, the cross-correlation of the two spectra peaks at  $\Delta V = (-0.05 \pm 0.11) \text{ km/s}$ , consistent with no velocity offset between the

lines. This yields  $[\Delta G/G] < 1.16 \times 10^{-5}$ , from  $z \sim 0.0018$ . This demonstrates the expected null result in a “local” comparison, at a sensitivity similar to that of the high- $z$  result.

The result for PKS 1413+135 can be used to obtain (model-dependent) constraints on both  $[\Delta\alpha/\alpha]$  and  $[\Delta\mu/\mu]$  by defining  $[\Delta\mu/\mu] = R[\Delta\alpha/\alpha]$ . This yields  $[\Delta\alpha/\alpha] \times (2 - R) = (+5.0 \pm 3.1) \times 10^{-6}$ , again assuming  $[\Delta g_p/g_p] \ll [\Delta\alpha/\alpha], [\Delta\mu/\mu]$ . Given a value of  $R$  from a theoretical model, one can immediately obtain an estimate for  $[\Delta\alpha/\alpha]$ . For example, values of  $R \sim -50$  are typical in GUT models (e.g. [4, 3]), giving  $[\Delta\alpha/\alpha] \lesssim \text{few} \times 10^{-7}$  (note that  $R$  can have either sign but is typically large in absolute value, in the absence of fine-tuning). Changes in  $G$  are then dominated by changes in  $\mu$ ; any model with  $|R| \gtrsim 10$  yields a similar result. This gives  $[\Delta\alpha/\alpha] < 8 \times 10^{-7}$  and  $[\Delta\mu/\mu] \lesssim 8 \times 10^{-6}$  from  $z \sim 0.247$ .

The above discussion also highlights the main drawback of the conjugate-satellites technique, the fact that it cannot be used to directly measure changes in individual constants (like the many-multiplet or  $\text{H}_2$  methods), but instead probes changes in a combination of three constants,  $\alpha$ ,  $\mu$  and  $g_p$ . Constraints on changes in the individual constants from this method are hence model-dependent (e.g. the assumption that  $g_p$  remains unchanged). [21] point out that, for the  $119\mu\text{m}$  decays, an over-population of the ground state  $F = 2$  sub-levels should be accompanied by an over-population of the  $F = 3$  sub-levels in the  $J = 5/2$  state, implying that the  $J = 5/2$  satellite lines should also be conjugate. Using these lines in tandem with the ground state satellite lines would reduce the degeneracy in the conjugate-satellites method between changes in  $\alpha$ ,  $\mu$  and  $g_p$  [59]. However, despite deep searches [58], the  $J = 5/2$  satellite lines have not so far been detected at cosmological distances.

The strength of the conjugate-satellites technique stems from the fact that the conjugate behaviour *guarantees that the satellite lines arise from the same gas*. Such systems are hence perfectly suited to probe changes in  $\alpha$ ,  $\mu$  and  $g_p$  from the source redshift to today, as systematic velocity offsets between the lines are ruled out by the inversion mechanism. Any measured difference between the line redshifts must then arise due to a change in one or more of  $\alpha$ ,  $\mu$  and  $g_p$  [21]. The technique also contains a stringent test of its own applicability, in that the shapes of the two lines must agree if they arise in the same gas. Further, it provides a estimate of changes in the fundamental constants from a single space-time location, without any averaging over multiple absorbers (which, for example, is essential in most other methods to average out local systematics). In addition, the velocity offset between the lines can be determined from a cross-correlation analysis, as the shapes of the lines are the same; it is not necessary to model the line profiles with multiple spectral components of an assumed shape, which can, especially for complex profiles, itself affect the result. As noted earlier, the use of masers of local oscillators to set the radio frequency scale means that frequency calibration is also not an issue here. Finally, the nearest isotopic OH transitions are more than 50 MHz away and this part of the radio spectrum has very few other known astronomical transitions; line

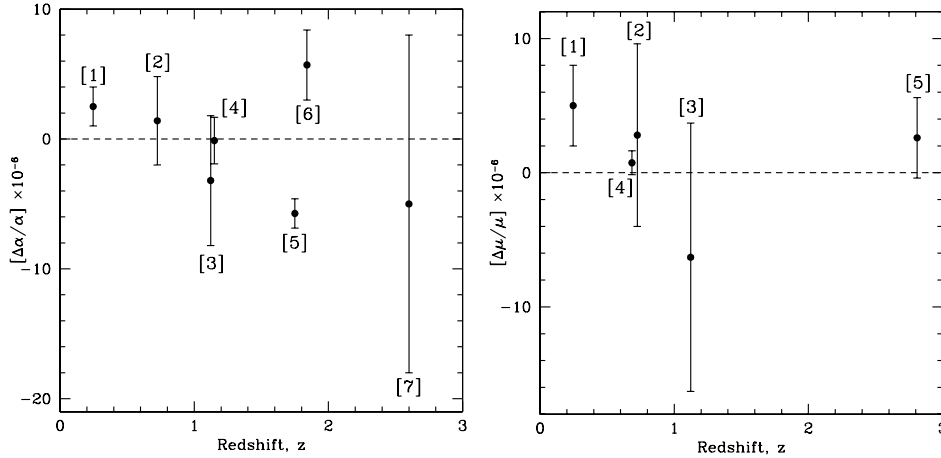


Fig. 2. Current results from techniques probing fundamental constant evolution with redshifted spectral lines. The left panel [A] shows the best present estimates for  $[\Delta\alpha/\alpha]$  as a function of redshift, from the [1] conjugate-satellites [58], [2] H<sub>i</sub> 21cm vs. OH lines [48], [3] H<sub>i</sub> 21cm vs. fine structure lines [42], [4] SIDAM, at  $z \sim 1.15$  [30], [5] MM [31], [6] SIDAM, at  $z \sim 1.84$  [30], and [7] AD [25], methods. Panel [B] shows similar results for  $[\Delta\mu/\mu]$ , from the [1] conjugate-satellites [58], [2] H<sub>i</sub> 21cm vs. OH lines [48], [3] H<sub>i</sub> 21cm vs. fine structure lines [42], [4] NH<sub>3</sub> vs. rotational lines [50], and [5] H<sub>2</sub>[40], methods. The assumptions  $[\Delta\alpha/\alpha] \gg [\Delta\mu/\mu]$ ,  $[\Delta g_p/g_p]$  (in [A]) and  $[\Delta g_p/g_p], [\Delta\alpha/\alpha] \ll [\Delta\mu/\mu]$  (in [B]) apply to the first three in each category. Note that the comparison between NH<sub>3</sub> and rotational lines assumes no local velocity offsets between the lines, while the H<sub>i</sub> 21cm vs. OH comparison uses a velocity dispersion of 3 km/s [48, 50].

interlopers are thus not likely to be an issue in this method, unlike the situation in the optical regime [58]. Overall, systematic effects appear to be far less important for the conjugate-satellites method than for the other techniques.

## 6. Results from the different techniques

It is difficult to directly compare results from radio and optical techniques as the former (except for the NH<sub>3</sub> lines) probe combinations of  $\alpha$ ,  $\mu$  and  $g_p$ . A model-dependent summary of the best present results can be obtained for the two limiting cases,  $[\Delta\alpha/\alpha] \gg [\Delta\mu/\mu]$  and  $[\Delta\alpha/\alpha] \ll [\Delta\mu/\mu]$ , assuming that  $[\Delta g_p/g_p] \ll [\Delta\alpha/\alpha], [\Delta\mu/\mu]$  (e.g. [4]). Such a comparison, between the alkali doublet, many-multiplet, SIDAM, H<sub>i</sub> 21cm vs. fine structure, H<sub>i</sub> 21cm vs. OH, NH<sub>3</sub> vs. rotational, conjugate-satellites and H<sub>2</sub> methods, is shown in the two panels of Fig. 2 [25, 29, 40, 42, 48, 58, 50]. It is apparent that present results from the conjugate-satellites, many-multiplet and SIDAM methods have similar sensitivities to changes in  $\alpha$ , although at very different lookback times. Conversely, the NH<sub>3</sub> method is the most sensitive among probes of changes in  $\mu$  (although note that [50] assume no local offsets between the NH<sub>3</sub> and rotational lines), with the conjugate-satellites and H<sub>2</sub> methods having similar sensitivities, albeit again at widely separated redshifts.

The figure also shows a clear separation between the redshift ranges at which the

radio and optical techniques have been applied. The optical techniques are all based on ultraviolet transitions that only move into optical wavebands (say,  $\gtrsim 3200\text{\AA}$ ) for absorbers beyond a certain redshift. This means that, for example, the  $\text{H}_2$  technique can only be used at  $z \gtrsim 2$ , the SiIV AD technique at  $z \gtrsim 1.3$  and the SIDAM method (using the FeII $\lambda$ 1608 line; [32]) at  $z \gtrsim 1$ . Similarly, only a handful of lines from singly-ionized species are redshifted above  $3200\text{\AA}$  at  $z \lesssim 0.6$ , implying that the many-multiplet method too works best at higher redshifts ( $z \gtrsim 0.8$ ). On the other hand, the lack of known radio molecular absorbers at  $z > 0.9$  limits the radio methods to relatively low redshifts. Present radio and optical techniques thus play complementary roles in studies of fundamental constant evolution, with the best low- $z$  measurements coming from radio wavebands and the best high- $z$  estimates, from the optical regime. It is also clear that the many-multiplet method is the only present technique that finds statistically significant evidence of changes in  $\alpha$  or  $\mu$ .

## 7. Future studies

The present limitations of the optical and radio techniques are very different in nature. The optical methods are affected by issues like line blending, relative calibration of different echelle orders, unknown relative isotopic abundances at high redshifts and the fact that it has not been possible to obtain an estimate of local systematic effects in the Galaxy. The biggest drawback to the radio methods is the paucity of high- $z$  radio absorbers, due to which one cannot average out local systematics (note that this does not affect the conjugate-satellites method).

Over the next decade, new telescopes and associated instrumentation will address some of these issues, at both radio and optical wavebands. The next generation of (30-metre-class) optical telescopes and new spectrographs should result in both improved spectral resolution (alleviating problems with line blends, especially useful for the  $\text{H}_2$  method) as well as much better wavelength calibration. However, even the planned spectrograph CODEX, with a resolving power of  $R \sim 150000$  (e.g. [60]), will be unable to resolve out the Mg isotopic structure (the different isotopic transitions are separated by only  $\sim 0.85$  km/s and  $\sim 0.4$  km/s for MgII $\lambda$ 2803 and MgI $\lambda$ 2853, respectively; [25]). Unknown relative isotopic abundances in the high- $z$  absorbers is thus likely to remain an issue for the MM (and SIDAM) methods, although statistical errors of  $[\Delta\alpha/\alpha] \sim 10^{-7}$  should be achievable. Additional corrections to the Born-Oppenheimer approximation may be necessary to improve the precision in the  $\text{H}_2$  method [39] to reach similar sensitivities in  $[\Delta\mu/\mu]$ . Finally, it is unlikely that it will be possible to test for a null result from these methods in the Galaxy, as this would require high-resolution ultraviolet spectroscopy.

On the other hand, increasing the number of redshifted systems detected in atomic and molecular radio lines is a critical ingredient for future radio studies of fundamental constant evolution. The wide-band receivers and correlators of the Green Bank Telescope, the Atacama Large Millimeter Array and the Expanded Very Large Array will, for the first time, allow “blind” surveys for redshifted absorption

in the strong mm-wave rotational transitions towards a large number of background sources. This should yield sizeable samples of high- $z$  absorbers in these transitions, which can then be followed up in other molecular and atomic lines. It should then be possible to average over local velocity offsets or different kinematic structures to obtain reliable results when comparing line redshifts across species. These surveys should also reveal a new population of redshifted conjugate satellite OH systems (note that two of the five known radio molecular absorbers show conjugate-satellite behaviour). Deep ( $> 100$  hour) integrations on the  $z \sim 0.247$  conjugate system in PKS 1413+135 with existing telescopes in the next few years should achieve  $1\sigma$  sensitivities of  $[\Delta\alpha/\alpha], [\Delta\mu/\mu] \sim \text{few} \times 10^{-7}$  while, in the long-term future, the Square Kilometer Array will be able to detect fractional changes of  $[\Delta\alpha/\alpha] \sim 10^{-7}$  in both known (and any newly-detected) conjugate systems.

It thus appears that similar sensitivity to fractional changes in  $[\Delta\alpha/\alpha]$  will be achievable with both the many-multiplet (or SIDAM) and conjugate-satellites methods over the next decade or so, although new conjugate systems will have to be detected at high redshifts to extend this method beyond  $z \sim 0.8$ . The lack of apparent systematic effects in the conjugate-satellites method suggest that it is likely to be the most reliable probe of fundamental constant evolution, unless the issue of unknown isotopic abundances in the MM method can be resolved. However, the drawback that the conjugate-satellites method is only sensitive to changes in a combination of  $\alpha$ ,  $\mu$  and  $g_p$  means that other approaches will be necessary to measure changes in these constants independently. In any event, it remains important that multiple techniques be used so as to ensure that the results are not affected by unknown systematic effects that could be specific to one method.

## 8. Summary

Optical and radio techniques have played complementary roles in extending studies of fundamental constant evolution to large lookback times. Optical approaches have provided high sensitivity at high redshifts,  $z \sim 0.8-3.0$ , while radio approaches have been critical to study the late-time ( $z \lesssim 0.8$ ) behaviour. The best present results, from a variety of methods, have  $2\sigma$  sensitivities of  $[\Delta\alpha/\alpha], [\Delta\mu/\mu] \sim \text{few} \times 10^{-6}$  at  $z \sim 0.25-2.8$ , an improvement of nearly two orders of magnitude in the last decade. The conjugate-satellites technique appears to have the fewest systematic effects of all methods considered here, with the agreement between the satellite OH line shapes providing a stringent test of its own applicability. The only technique yielding statistically-significant evidence for changes in the fundamental constants remains the many-multiplet method [31], which finds a smaller value of  $\alpha$  at early times. While it has still not been possible to definitely confirm or deny this result, much progress has been made in developing new techniques and understanding systematic effects. It is important to continue such studies with a range of techniques, both to ensure that the results are not dominated by systematic effects in any given approach and to probe changes in multiple constants over a wide range of redshifts.

## 9. Acknowledgments

It is a pleasure to thank Jayaram Chengalur and Carlos Martins for stimulating discussions on fundamental constant evolution and comments on an earlier draft, Jayaram and Tapasi Ghosh for permission to discuss our unpublished results, and Huib van Langevelde for providing us with the OH spectra towards Cen.A. I acknowledge support from the Max Planck Foundation and an NRAO Jansky Fellowship.

## References

1. W. J. Marciano, Phys. Rev. Lett. **52**, 489 (1984).
2. T. Damour and A. M. Polyakov, Nucl. Phys. B **423**, 532 (1994).
3. X. Calmet and H. Fritzsch, Eur. Phys. Jour. C **24**, 639 (2002).
4. P. G. Langacker, G. Segré, and M. J. Strassler, Phys. Lett. B **528**, 121 (2002).
5. T. Rosenband *et al.*, Science **319**, 1808 (2008).
6. A. Shelkovich, R. J. Butcher, C. Chardonnet, and A. Amy-Klein, Phys. Rev. Lett. **100**, 150801 (2008).
7. J.-P. Uzan, Rev. Mod. Phys **75**, 403 (2003).
8. Y. Fujii and A. Iwamoto, Phys. Rev. Lett. **91**, 261101 (2003).
9. C. R. Gould, E. I. Sharapov, and S. K. Lamoreaux, Phys. Rev. C **74**, 024607 (2006).
10. Y. V. Petrov *et al.*, Phys. Rev. C **74**, 064610 (2006).
11. E. W. Kolb, M. J. Perry, and T. P. Walker, Phys. Rev. D **33**, 869 (1986).
12. S. Hannestad, Phys. Rev. D **60**, 023515 (1999).
13. M. Kaplinghat, R. J. Scherrer, and M. S. Turner, Phys. Rev. D **60**, 023516 (1999).
14. M. P. Savedoff, Nature **178**, 688 (1956).
15. G. Rocha *et al.*, MNRAS **352**, 20 (2004).
16. T. Dent, S. Stern, and C. Wetterich, Phys. Rev. D **76**, 063513 (2007).
17. J. N. Bahcall, C. L. Steinhardt, and D. Schlegel, ApJ **600**, 520 (2004).
18. T. Wiklind and F. Combes, A&A **328**, 48 (1997).
19. C. L. Carilli *et al.*, Phys. Rev. Lett. **85**, 5511 (2000).
20. V. A. Dzuba, V. V. Flambaum, and J. H. Webb, Phys. Rev. Lett. **82**, 888 (1999).
21. N. Kanekar, J. N. Chengalur, and T. Ghosh, Phys. Rev. Lett. **93**, 051302 (2004).
22. J. Darling, ApJ **612**, 58 (2004).
23. J. N. Bahcall, W. L. W. Sargent, and M. Schmidt, ApJ **149**, L11 (1967).
24. A. V. Ivanchik, A. Y. Potekhin, and D. A. Varshalovich, A&A **343**, 439 (1999).
25. M. T. Murphy *et al.*, MNRAS **327**, 1237 (2001).
26. H. Chand, R. Srianand, P. Petitjean, and B. Aracil, A&A **430**, 47 (2005).
27. M. T. Murphy, J. K. Webb, and V. V. Flambaum, MNRAS **384**, 1053 (2008).
28. M. T. Murphy *et al.*, MNRAS **327**, 1223 (2001).
29. M. T. Murphy, J. K. Webb, and V. V. Flambaum, MNRAS **345**, 609 (2003).

30. P. Molaro, D. Reimers, I. I. Agafonova, and S. A. Levshakov, arxiv/0712.4380 (2007).
31. M. T. Murphy *et al.*, in *Astrophysics, Clocks and Fundamental Constants*, Vol. 648 of *Lecture Notes in Physics*, eds. S. G. Karshenboim and E. Peik (Springer-Verlag, Berlin, 2004), p. 131.
32. R. Quast, D. Reimers, and S. A. Levshakov, *A&A* **415**, L7 (2004).
33. S. A. Levshakov *et al.*, *A&A* **466**, 1077 (2007).
34. H. Chand, R. Srianand, P. Petitjean, and B. Aracil, *A&A* **417**, 853 (2004).
35. T. P. Ashenfelter, G. J. Mathews, and K. A. Olive, *ApJ* **615**, 82 (2004).
36. Y. Fenner, M. T. Murphy, and B. K. Gibson, *MNRAS* **358**, 468 (2005).
37. R. I. Thompson, *ApL* **16**, 3 (1975).
38. D. A. Varshalovich and S. A. Levshakov, *JETP* **58**, L237 (1993).
39. E. Reinhold *et al.*, *Phys. Rev. Lett.* **96**, 151101 (2006).
40. J. A. King, J. K. Webb, M. T. Murphy, and R. F. Carswell, arxiv/0807.4366 (2008).
41. A. M. Wolfe, J. J. Broderick, J. J. Condon, and K. J. Johnston, *ApJ* **208**, L47 (1976).
42. P. Tzanavaris *et al.*, *MNRAS* **374**, 634 (2007).
43. N. Kanekar *et al.*, *MNRAS* **370**, L46 (2006).
44. C. L. Carilli, K. M. Menten, M. J. Reid, and M. P. Rupen, *ApJ* **474**, L89 (1997).
45. T. Wiklind and F. Combes, *A&A* **315**, 86 (1996).
46. N. Kanekar and J. N. Chengalur, *MNRAS* **384**, L6 (2008).
47. J. N. Chengalur and N. Kanekar, *Phys. Rev. Lett.* **91**, 241302 (2003).
48. N. Kanekar *et al.*, *Phys. Rev. Lett.* **95**, 261301 (2005).
49. V. V. Flambaum and M. G. Kozlov, *Phys. Rev. Lett.* **98**, 240801 (2007).
50. M. T. Murphy, V. V. Flambaum, S. Muller, and C. Henkel, *Science* **320**, 1611 (2008).
51. C. Henkel *et al.*, *A&A* **440**, 893 (2005).
52. T. Wiklind and F. Combes, in *Highly Redshifted Radio Lines*, eds. C. L. Carilli *et al.* (Astronomical Society of the Pacific, 1999), Vol. 156, p. 202.
53. M. Elitzur, *Astronomical masers* (Kluwer Academic, Dordrecht, NL, 1992).
54. H. J. van Langevelde, E. F. van Dishoek, M. N. Sevenster, and F. P. Israel, *ApJ* **448**, L123 (1995).
55. E. R. Hudson, H. J. Lewandowski, B. C. Sawyer, and J. Ye, *Phys. Rev. Lett.* **96**, 143004 (2006).
56. B. L. Lev *et al.*, *Phys. Rev. A* **74**, 061402 (2006).
57. J. Darling, *Phys. Rev. Lett.* **91**, 011301 (2003).
58. N. Kanekar *et al.*, in preparation (2008).
59. N. Kanekar and J. N. Chengalur, *MNRAS* **350**, L17 (2004).
60. P. Molaro, M. T. Murphy, and S. A. Levshakov, in *The Scientific Requirements for Extremely Large Telescopes*, eds. P. Whitelock *et al.* (Cambridge University Press, Cambridge, 2006), p. 198.